HHS Public Access

Author manuscript

Clin Psychol Sci. Author manuscript; available in PMC 2016 May 01.

Published in final edited form as:

Clin Psychol Sci. 2015 May 1; 3(3): 422–432. doi:10.1177/2167702614562042.

Single stimulus fMRI produces a neural individual difference measure for Autism Spectrum Disorder

James Lu[3,4,5,*], **Ken Kishida**[1,*], **Josepheen De Asis Cruz**[6,*], **Terry Lohrenz**[1], **Diane Treadwell Deering**[7], **Michael Beauchamp**[8], and **P Read Montague**[1,2,3,9]

[1]Virginia Tech Carilion Research Institute, Virginia Tech, Blacksburg VA

[2]Department of Physics, Virginia Tech, Blacksburg VA

[3]The Wellcome Trust Centre for Neuroimaging, University College London, London, UK

[4]Human Genome Sequencing Center, Baylor College of Medicine, Baylor College of Medicine, Houston, TX

[5]Department of Structural and Computational Biology and Molecular Biophysics, Baylor College of Medicine, Houston, TX

[6]Department of Neuroscience, Baylor College of Medicine, Houston TX

[7]Menninger Department of Psychiatry and Behavioral Sciences, Baylor College of Medicine, Houston, TX

[8]Department of Neurobiology and Anatomy, University of Texas Health Science Center, Houston, TX

Abstract

Functional magnetic resonance imaging typically makes inferences about neural substrates of cognitive phenomena at the group level. We report the use of a single-stimulus BOLD response in the cingulate cortex that differentiates individual children with autism spectrum disorder from matched typically developing control children with sensitivity and specificity of 63.6% and 73.7% respectively. The approach consists of passive viewing of ‘self’ and ‘other’ faces from which an individual difference measure is derived from the BOLD response to the first ‘self’ image only; the method, penalized logistic regression, requires no averaging over stimulus presentations or individuals. These findings show that single-stimulus fMRI responses can be extracted from individual subjects and used profitably as a neural individual difference measure. The result suggests that single-stimulus fMRI can be developed to produce quantitative neural biomarkers for other developmental disorders and may even be useful in the rapid typing of cognition in healthy individuals.

Address correspondence to: James T. Lu, Baylor College of Medicine – Human Genome Sequencing Center One Baylor Plaza MS: BCM226 Houston Texas 77030 United States, jtlu@bcm.edu.

[9]Corresponding author – read@vt.edu

[*]These authors contributed equally to this work

Authorship Statement

JTL performed the analysis and wrote and revised the manuscript. KK planned the experiment, assisted with analysis and revised the manuscript. JDAC performed the experiments and analysis and revised the manuscript. TL, DTD, and MB supervised the experiment, assisted with analysis and revised the manuscript. PRM assisted with experimental design, analysis, and revision of the manuscript.

Functional magnetic resonance imaging has become a major tool in cognitive neuroscience where cognitive variables are correlated with blood oxygenation level (BOLD) measurements throughout the brain to identify spatiotemporal neural dynamics associated with variable(s) of interest (Huettel, Song, & McCarthy, 2008). This general approach is carried out almost exclusively in terms of averages of BOLD responses over multiple presentations of stimuli because of relatively low signal-to-noise issues in the raw BOLD signal. Averaging within a single individual is often followed by averaging across individuals to generate group level summaries about neural responses to stimuli. The presumed need for averaging presents one barrier to using fMRI as a method for generating rapid, individual difference responses useful for characterizing healthy or diseased cognition. Moreover, the intrinsic sluggishness and spatial imprecision of the BOLD response contributes to the general perception that fMRI is a useful neuroimaging modality only in 'averaging mode'. Here we present new results that suggest that this view is incomplete and that fMRI can be used to generate a single stimulus measurement useful as an individual difference measure and biomarker in one of the most common neurodevelopmental disorders – autism spectrum disorder (ASD).

Our investigation of the possibility of using a single-stimulus approach in ASD stems from extensive prior work, which demonstrated that the middle cingulate cortex is particularly responsive during social exchange in a manner that is consistent with the hypothesis that this region is important for cognitive processes related to perspective taking. Specifically, Tomlin et al., showed that activity in the cingulate cortex tracks the active agent (i.e., "me" versus "not me") during a social exchange experiment involving 100 pairs of participants (Tomlin et al., 2006). Following this work, Chiu and colleagues demonstrated that one of these agent-specific responses (the "self-response") in the middle cingulate cortex was diminished in individuals diagnosed with Autism Spectrum Disorder (Chiu et al., 2008). Chiu et al., also showed that diminished responses in the middle cingulate cortex were positively correlated with symptom severity in the ASD cohort (Chiu et al., 2008). In the same report, Chiu and colleagues also performed a visual imagery experiment using 81 accomplished athletes and 27 healthy adult. During an eyes-closed mental imagery task, these participants showed that the same pattern of activity (i.e., "self-response" along the cingulate cortex) could be elicited during eyes-closed mental imagery of the first-person perspective, but not during third-person perspective taking (Chiu et al., 2008)., Kishida and colleagues hypothesized that the region of the middle cingulate that was engaged during perspective taking, social exchange, and was diminished in the ASD cohort could be specifically activated by showing participants pictures of themselves (Kishida, Li, Schwind, & Montague, 2012). Using a passive picture viewing task in healthy adults and the region of interest defined in the eyes closed mental imagery task, Kishida et al., (Kishida et al., 2012) showed in an adult cohort that indeed the middle cingulate cortex differentiated pictures of "self faces" from pictures of "other faces".

Taken together, these results suggested the hypothesis that a similar picture viewing assay might elicit signals in this same region-of-interest strong enough to produce a neural measure that might also differentiate children diagnosed with ASD from age-matched typically developing (TD) children (cohort level statistics are provided in Table S2). We

also included adult controls to ensure consistency with past findings. We designed a full-length passive picture-viewing paradigm to test this hypothesis; however, two empirical findings suggested the necessity of exploring a reduced experimental design. First, the duration of the full-length experiment (~12 minutes) proved too long for children diagnosed with ASD to remain still in the fMRI scanning environment; second, in TD children, an effect consistent with repetition suppression of BOLD responses in the MCC to repeated presentations of self and other images suggested that an 'average brain response' to multiple presentations is very different than responses to a more reduced design. Following these results we tested the most extreme version of a 'reduced experimental design' and demonstrate that a machine learning approach and single stimulus fMRI data from an *a priori* prescribed region-of-interest can produce results consistent with a rapidly assessable individual difference measure for autism spectrum disorder.

Results

In a passive viewing paradigm, adults and children (typically developing, TD and diagnosed with autism spectrum disorder, ASD) were shown 15 presentations each of images of themselves ("self") and an age- and sex-matched individual ("other"; Figure 1a). These images were presented in a randomized order such that the starting image for each subject occurs by chance. BOLD responses to "self" and "other" image presentations were then extracted using the "eyes closed mental imagery" ROI in the middle cingulate cortex (Figure 1b, inset image from Kishida et al.,). Consistent with previous findings by Kishida et al., adults (n=33) in this study showed greater response to self-faces than to other-faces with averaging of all presentations (data not shown) and with a single stimulus response (Figure S3).

In analysing data for TD and ASD individuals we focused on the hemodynamic response to the first presentation of either "self" or "other stimuli for two reasons: 1) repetition suppression and 2) task length. Repetition suppression is the reduction of neural responses to repeated stimuli due to stimulus recognition and learning (Grill-Spector, Henson, & Martin, 2006; Henson & Rugg, 2003; Segaert, Weber, de Lange, Petersson, & Hagoort, 2013). In our experimental paradigm, repetition suppression of the BOLD signal was evident by the second image presentation (Figure S1a). In our study, we found in Adults (data not shown), TD (Figure S2a) and ASD (Figure S2b) that cohort level differences in peak hemodynamic response for "self" and "other" images were maximal after the first stimulus presentation and did not improve with multiple presentations (See Supplement).

In addition, we found that longer experimental paradigms reduced the cohort of individuals that were available for analysis. Using a instantaneous movement threshold of ±3.5mm, we plot a Kaplan Meier curve for experimental completion for all participating subjects (Figure S3) by total scanning time. Our task was approximately 12 minutes total length. Unlike adult and TD subjects, which are able to voluntarily lie still for extended periods of time, ASD children showed significant head movement. After 5 minutes of scanning time, over 40% of the data from the ASD population could not be analysed to due excessive head movement. However by reducing scanning time to less than 2 minutes, i.e. "single stimulus" responses, we could retain over 75% of the ASD participants.

The challenges associated with full length experiments in children diagnosed with ASD motivated the exploration of a reduced experimental design – in the extreme, eliciting a reliable brain response to a single stimulus would provide dramatically increased flexibility in the kinds of fMRI experiments that could be designed. In figure 2 (and figure S3), the cohort level hemodynamic response to the first presentation of a “self” image is displayed alongside the analogous time series for the first presentation of the “other” image for TD (n=38; Figure 2a), ASD (n=22; Figure 2b), and adult subjects (n=33; Figure S3). These data show two clear features at the cohort level. First, single stimulus responses elicit a large BOLD response in the cingulate cortex. In the TD cohort, the peak hemodynamic response differentiates between self versus other face (p=0.04, right sided t-test) (Figure 2a and 2c), consistent with analyses in adults in this study (p=0.03, respectively, right sided t-test, Figure S3), and previously reported findings in adults (Kishida et al., 2012). Secondly, unlike TD children, single-stimulus peak BOLD responses in the ASD cohort did not differentiate “self” from “other” images (p=0.16, right sided t-test). When comparing the TD and ASD cohorts, peak responses to “self” images differentiated the TD cohort and ASD cohorts (p= 0.04, right sided t-test) but responses to “other” images did not (p=0.22, right sided t-test). Thus differences across the two populations arose specifically for the time series responses for the ‘self’ picture (Figure 2c).

To test whether TD and ASD subjects were actively viewing the face image stimuli we extracted responses from bilateral fusiform face area (FFA) in 21 control adults in a separate task using a passive viewing paradigm of faces and objects (Figure S5) following (Kanwisher & Yovel, 2006). Using a general linear model (GLM) contrast, we assessed visual responses in the fusiform gyrus with particular attention to the fusiform face area to determine whether participants viewed the images. We found that the bilateral FFA, activates robustly in both cohorts in response to “self” and “other” face images. While some studies report decreased FFA activity in ASD patients (Deeley et al., 2007; Humphreys, Hasson, Avidan, Minshew, & Behrmann, 2008), others showed that familiarity (Pierce, Haist, Sedaghat, & Courchesne, 2004), age (Pierce & Redcay, 2008), and attention (Hadjikhani et al., 2004) engage the FFA in autism. The lack of differences in FFA activation between TD and ASD children (Figure S5) during image presentations suggests that both cohort’s brains detected the face images throughout the task (p_{unc}<0.005, k=10) (Pessoa, McKenna, Gutierrez, & Ungerleider, 2002).

Across the ASD and TD cohorts, the hemodynamic time series differences to “self” images (Figure 2a,b) provided an opportunity to develop an individual difference measurement, i.e. a single parameter value that summarizes an individual’s BOLD response time series to a single stimulus “self” image (Figure 3). One simple approach is to discriminate the control and diseased population using the peak response. Discriminant classification of disease status based solely on the percentage signal change in the peak activation of the BOLD response resulted in sensitivity and specificity of 54.6% and 57.9% respectively and an AUC of 0.591 (Figure 4a, Figure S6); this is a subpar classification of disease state for individuals. However, we show that we can improve classification by including more data from the time series. Focusing only on data captured by a peak hemodynamic response discards information encoded elsewhere in the dynamics of the ROI response. In addition, the hemodynamic response to any stimulus already has included a profound smoothing effect

that is compounded by further averaging. To improve classification we utilized the information of an entire time series in the pre selected region-of-interest and employed a penalized logistic regression. This classification method generates, for each time series sample following a self picture presentation, the probability of being assigned to the ASD group ex: $p(status = ASD \mid M)$, given the model (M).

In ordinary logistic regression the objective function is the cross entropy loss (see Supplemental information) (Bishop, 2006). While this method is commonly used and results in low bias classification, models that include a large number of covariates often have high variance due to over-fitting. Such over-parameterized models can have low prediction accuracy for future datasets (Tibshirani, 1996). Accordingly, we used a variable selection technique that employs an L1 penalization, which shrinks some coefficients and sets others to zero. One variation of this method is called the "least absolute shrinkage and selection operator" or LASSO. The LASSO objective function includes a penalty term, λ, which is a non negative regularization parameter (Count, 2010) (see Methods). Akin to choosing the number of predictors in a regression model, λ is changed to increase or decrease the number of nonzero, p, components. Larger values of λ result in more β coefficients being set to zero. The value of λ that minimizes misclassification error can be computed using K fold cross validation. Penalization created a 'reduced' model that excluded covariates that do not affect the outcome variable. Practically, if a model contains multiple correlated covariates, as we would expect for time-series data, most coefficients will be set to zero (See Supplemental Methods for more detail).

We used age, a "First or Not First" (FNF) covariate that indicates whether the first stimulus was also the starting image, and the time series data for the BOLD response for the "self" image, as 12 covariates in our model. To evaluate classification, we initially performed a logistic regression using a standard general linear model package in R. As expected, the full model is over-parameterized due to autocorrelation resulting in poorly estimated parameters (Table 1a), and is difficult to interpret. Area under the curve (AUC), for the receiver-operating curve (ROC) for this 'full' model was, 0.817 (Figures 4a). To improve parameter estimation, we employed leave-one-out cross–validation (LOOCV) and penalization to identify a model that minimizes misclassification (Friedman, Hastie, & Tibshirani, 2010). We found that the optimal model reduced the number of covariates to 12 to 8 (Figure 4b). AUC for this 'reduced' model was 0.773 (Figure 4c) and sensitivity and specificity for this model are 63.6% and 73.7% respectively (Table 1b). The coefficients emphasize not only the difference in amplitude in self-responses, but also differences in the relaxation and latency of the BOLD response (Figure 2a,b). Evaluating misclassification error for different numbers of variables revealed that the penalized model would have similar expected misclassification error on future datasets as a full model (Figure 4b). The computed individual difference measurements for each individual can be aggregated into separate distributions; D-prime (D') between the two cohorts was computed to be 1.50 in the reduced model (Figure 4d).

To evaluate the specificity of our response to the single-stimulus "self" image, we also employed the procedure to the BOLD time series for the first presentation of the "other" image. After applying the same LOOCV and penalization we found that the generated

model did not include any time-series information from the "other" images (coefficients were set to zero) (Figure S7a). This model only included a constant and the "age" covariate. This model generated a ROC curve with an AUC of 0.607, marginally better than chance (Figure S7b). These results are consistent with (though not definitive) the specificity of self-faces but not other-images for eliciting differentiating responses in the MCC across TD and ASD individuals.

Discussion

ASD is a highly heterogeneous (Lichtenstein, Carlström, Råstam, Gillberg, & Anckarsäter, 2010; Schaaf & Zoghbi, 2011) disorder with concomitant diagnostic complexities. Neuroimaging and neuropathology studies have revealed that brain growth and organization in ASD is fundamentally different (Johnson & Myers, 2007), thus usage of magnetic resonance imaging (MRI) as a biological assay holds great interest as a supplement to current diagnostic techniques. Studies to classify normally developing and ASD children have utilized anatomical differences in grey and white matter volume (Neeley et al., 2007) and cortical thickness (Jiao et al., 2010), and whole brain pattern classification (Ecker et al., 2010). Like many of these previous proof-of-concept studies exploring alternative assays to diagnose ASD, our study is not powered to evaluate test and retest reliability.

Prior fMRI work has relied primarily on averaging over multiple presentations to determine group level responses to stimuli. To our knowledge this is the first fMRI experiment to exploit a single stimulus induced BOLD time series that also produced a neural individual difference measure. The literature (Henson & Rugg, 2003) and our data (discussed above) suggest that it is not yet clear how the meaning of a stimulus changes with repeated presentations within a subject's experimental trial. Our successful elicitation of a single-stimulus result in part relies heavily on our prior work defining the region of interest, the cognitive variable, and their relationship to the population of interest. We present evidence of repetition suppression in our region-of-interest, which begins to occur by the second presentation. Minimally, these results imply unanswered questions about how the cognitive interpretation of a stimulus changes over repeated presentations and how brain responses change respectively. Future work will be needed to further explore the difference between single and multiple presentation paradigms.

Although our measurement provided a moderate to high discrimination, we in fact, expected that a proportion of ASD and TD samples would be misclassified. First, hemodynamic responses to stimuli vary across the population and our study numbers are not powered to properly map this variation. Second, the MCC has been linked to "perspective-taking" in individuals (Lombardo et al., 2010), an ability that matures with age (Mitchell & O'Keefe, 2008; Sally & Hill, 2006). One plausible interpretation is that the conflation of disease status and cognitive maturation hamper our ability to discriminate between ASD and TD individuals. Third, while our measurement may map loosely onto current DSM IV clinical criteria for ASD, in particular the axis regarding poor social interaction, these axes leave substantial room for interpretation and have already changed in DSM V. Lastly, given the heterogeneity in ASD presentations (Ronald et al., 2006), we suspect that the most relevant

finding in this single stimulus experiment may be the relatively low misclassification rate of putatively typically developing children.

Several studies have explored the sensitivity and specificity of well-known ASD surveys Autism Diagnostic Observation Schedule (ADOS) and Autism Diagnostic Interview-Revised (ADI-R), diagnosis of ASD in comparison to “gold standard” clinical assessment (Gray, Tonge, & Sweeney, 2008; Ventola et al., 2006). In these studies, patients suspected (by survey) of ASD have yielded sensitivity of and specificity of 0.88–0.99 and 0.67–0.82 (ADOS), and 0.53–0.77 and 0.61–0.70 (ADI-R) respectively. While our results appear comparable at first glance, our results may be skewed favourably by selection and model bias. Namely our enrolled subjects are already diagnosed with ASD by “gold standard” clinical assessment, while evaluations of ADOS/ADI-R are conducted on suspected patients with blinded physicians. Proper external validation of this paradigm and model will require a large subject pool recruited using a screening tool, blinding of the evaluating physicians, and model validation using an external cohort, not just cross-validation.

The clinical adoption of a magnetic resonance imaging (MRI) biomarker for psychopathology will require, at minimum, reliable and accurate classification of disease. Further, the success of any potential clinical diagnostic strategy also depends on operational reliability, reliability that often derives from simple and cost-effective procedures. Although the simplicity and brevity of single-stimulus paradigms should reduce operator variability, this question has not been adequately explored. Our work suggests that single stimulus methodologies, in a MCC ROI that was previously identified in several hundred normal individuals in other “self” and “other” tasks (Chiu et al., 2008; King-Casas et al., 2005; Kishida, King-casas, & Montague, 2011; Tomlin et al., 2006), may provide accurate classification of disease in ASD patients. Further, BOLD time series data from simple and short paradigms, which had previously been thought to be highly smoothed and noise-ridden, may nonetheless provide useful diagnostic information. We are cautiously optimistic that this work may provide a small step toward developing MRI based applications for screening of psychopathology or other-more typical-cognitive phenotypes.

Methods

Stimuli

Photographs of subjects were taken prior to scanning. Subjects were draped around the shoulders to ensure image uniformity. They were instructed to gaze directly at the camera while assuming different head angles. Head angle was varied to reduce habituation to repeated presentations of face images. In the scanner, each participant was shown 15 pictures of the subject (‘self’), and 15 unique pictures of an age- and gender-matched individual (‘other’) (Figure 1) for four seconds. A computer-controlled projector was used to generate the images that were displayed to subjects using an overhead mirror mounted on the radiofrequency coil. Images were shown for 4 seconds in random order with random inter stimulus intervals drawn from a Poisson distribution with parameter value (λ) equal to 14 seconds. As such the starting image for each subject is randomized. Subjects were instructed to focus on the faces or on the white fixation cross (displayed during the inter-stimulus window). Only TD subjects were used as ‘other’ (i.e. control) images.

Participants

We recruited 39 adults with no known neuropsychiatric disorders, 51 TD children and 35 children with ASD (Table S2) from the Houston metropolitan area by word of mouth and advertisements. In addition ASD participants were also referred from the Texas Children's Hospital's Autism Center; after initial assessment using basic fMRI exclusion criteria, the remaining qualified subjects (n=45 TD, and n=27 ASD) were invited to Baylor College of Medicine (BCM) for familiarization with the scanning environment, scanning and assessments. Autism Diagnostic Observation Schedule (ADOS) scores were available for 20 of the 27 children (Lord, C., Rutter, M., DiLavore, P. D., & Risi, 2001). In 12 of these 20 subjects, the diagnoses was reconfirmed by the Autism Diagnostic Interview – Revised (ADI-R) (Le Couteur, A., Lord, C., & Rutter, 2003). The remaining seven of 20 patients were evaluated in autism centers at tertiary hospitals and diagnosed based on clinical presentation and developmental history. Lastly scores from the Social Responsiveness Scale (SRS) (Constantino & Todd, 2003), and Kaufman Brief Intelligence Test, Second Edition (KBIT-2) (Kaufman AS, 2004) were obtained for a subset of ASD and TD subjects (Table S2). The institutional review board at BCM approved the study protocol. Parents signed informed written consent and children provided assent.

Image Acquisition

Imaging was performed using a 3-T Siemens Allegra head only scanner and 3-T Siemens Trio full-body scanner. More specifically, 39 out of the 45 TD children and 26 out of the 27 ASD children were scanned in the Trio scanner. An analysis of peak differences between and within ASD and TD populations showed that no differences in hemodynamic responses were found to be attributable to the employed scanner. A localizer image was acquired first followed by high-resolution T1-weighted structural images (192 slices; in plane resolution: 256 × 256; field of view: 245 mm; slice thickness: 1 mm). Continuous whole-brain imaging was then performed as subjects viewed self and other faces on the screen. Regional brain activation was measured using changes in blood oxygen level dependent (BOLD) fMRI signal. The parameters for the functional sequence are as follows: echo-planar imaging, gradient recalled echo; repetition time = 2000ms; echo time = 30ms; flip angle = 90; 64 × 64 matrix (in-plane resolution); 34 4 mm axial slices positioned 30° to the anterior commissure/posterior commissure line.

Data were preprocessed and analyzed using the SPM8 software package (http://www.fil.ion.ucl.ac.uk/spm/software/spm8/) (Friston, Penny, Ashburner, Kiebel, & Nichols, 2006). During preprocessing, functional brain images were temporally realigned using linear interpolation to correct for variability in the timing of slice acquisition, spatially realigned using a six-parameter rigid-body transformation to correct for head movements, and co-registered onto high-resolution/high-contrast structural images. In adults, images are typically spatially normalized to a Montreal Neurological Institute template (MNI; SPM's EPI template) by applying a 12-parameter affine transformation to facilitate inter-subject comparison.

For the children in our study we generated customized T1 template and tissue probability maps (i.e. gray matter, white matter and cerebrospinal fluid priors) using the SPM8 toolbox

Template-O-Matic (https://irc.cchmc.org/software/tom.php). This toolbox is based on data obtained from 404 children as part of the normal brain development study of the National Institutes of Health (Wilke, Holland, Altaye, & Gaser, 2008). The toolbox takes in the ages and gender of the sample population as input and automatically generates references images based on parameters obtained from the NIH cohort. Children's images were then segmented and normalized using the unified segmentation model. During normalization, bounding box parameters of structural and functional images were matched to the adult masks to ensure that image dimensions and origin were the same. Normalized images, in all cohorts, were then spatially smoothed using an 8 mm Gaussian kernel and temporally filtered (cut-off period of 128s).

ROI Analysis

ROI analysis was performed using independently identified MCC voxels (Figure 1a, inset) from (Kishida et al., 2012). This MCC ROI, which was generated from adult patients, was resliced to our custom children's template using nearest neighbour interpolation. We have included in the Supplement, axial, coronal, and sagittal cuts of the ROI overlaid on the standard adult template and on our child templates generated with the Template-O-Matic toolbox (Figure S8). Raw time courses for this ROI were extracted using SPM functions, detrended and then averaged. Time series were captured for the period 6 seconds prior to stimulus presentation to 16 seconds post-stimulus presentation including the 4-second presentation interval. Data in this period were linearly interpolated (Matlab function interpl.m). Time series were captured for the first presentation of 'self' image and 'other images for each individual. BOLD responses were presented as percentage signal change from baseline BOLD rates (−6s to 0s, where t=0 is the stimulus presentation). The peak activation was defined as the mean response 6s to 8s post stimulus presentation relative to the response measured just prior to the stimulus onset (−6s to 0s).

Participant Inclusion Criteria

One adult of 39 was excluded because of technical problems during image acquisition (adults: n = 38, 14 males: 24 females; mean age = 29.9 ± 9.5 years old). Of the 51 TD, children, six were initially excluded from analysis: two, because of technical problems during scanning; one, due to subject's decision to discontinue with the study; one, because the subject fell asleep during the task, and; three, because of excessive head movement (> 3.5 mm), resulting in 37 TD subjects. Out of the 35 subjects with ASD, eight were initially excluded (27 remaining) from the analysis: one because of atypical brain morphology; five because of excessive head movement (inclusion criteria were instantaneous head motion ±3.5 mm 6s pre- and 16s post-stimulus onset for the first presentation of self and other picture); and two, because technical issues related to scanning prevented recording of these subjects' brain responses to the first stimulus presentation.

For the region of interest (ROI) analysis, a second inclusion criterion was used to remove hyper-variable hemodynamic responses to ensure data quality. Subjects with high MCC signal variability on the first presentation of self or other image were excluded to ensure that outlier values do not dominate the BOLD response and confound the results. Removal of

BOLD responses that may be contaminated with noise can be especially important when looking at a “single-stimulus” response.

Signal variability was measured as the standard deviation of the BOLD time course from seconds 6 seconds prior to presentation to 16 seconds post presentation. Outliers for signal variability were defined as having values in the signal greater than median (of population) ± 3 × IQR (inner quartile range) for all hemodynamic responses (Figure S9, Table S3). As signal variation in ASD and TD children were not statistically different (data not shown), these data were combined and analysed as a single “child” population”. Subjects with MCC signal standard deviation greater than 0.80% for TD and ASD subjects and 0.53% for Adults were removed from our “single-stimulus” ROI analysis. Thus, 33 of 38 adults, 38 of 44 TD children and 22 of 27 ASD children were retained for our ROI analysis. Excluded individuals did not have “single-stimulus” hemodynamic trajectories that resemble typical BOLD responses (Figure S10). In fact many appear to have large negative inflections or a sinusoidal pattern. Incidentally, all individuals who were excluded for variable “self” responses were also independently excluded for high variability “other” responses. This finding further reinforced the hypothesis that these BOLD trajectories were due to a common factor such as head movement (Power, Barnes, Snyder, Schlaggar, & Petersen, 2012) or some other unknown factor.

Classifier Development for Penalized Regression Model

Penalized regressions was computed using the glmnet package (Friedman, Hastie, Höfling, & Tibshirani, 2007; Friedman et al., 2010; Tibshirani, 1996) (R 2.15.1). ROC curves were plotted on Matlab 2012b using the perfcurve function. Before computing parameter values we first reweighted the value of individual samples such that the optimization uses ostensibly equal sized populations. Given our sample numbers of 38 TD and 22 ASD, this was akin to increasing the value of each ASD sample by 1.72 (38/22). Reweighting the samples and improves sensitivity and specificity of the classifier for the minor population (Cramer, 2013).

Penalized regression is a variable selection technique that shrinks some coefficients and sets others to zero. The least absolute shrinkage and selection operator, or *lasso* function, is a variable selection technique that utilizes an L^1-norm penalty. The L^1-norm penalty, alters the standard cross entropy loss objective function (See Supplement) to the following:

$$E(w) = -\sum_{n=1}^{N} \{y_n ln\sigma(\boldsymbol{X\beta}) + (1-y_n) ln(1-\sigma(\boldsymbol{X\beta}))\} - \lambda \sum_{k=1}^{p} |\beta_k|$$

λ is a nonnegative regularization parameter, or amount of penalization (Count, 2010). Akin to choosing the number of predictors in a regression model, λ is changed to increase or decrease the number of nonzero components. Larger values of λ result in more β coefficients being set to zero. The value of λ that minimizes misclassification error can be computed using K-fold cross validation (Friedman et al., 2007) (Figure S11).

Cross Validation

Cross-validation for different levels of penalization also allows us to visualize how models with different amounts of covariates were perform on independent datasets. In K-fold cross-validation (Bishop, 2006), the data is partitioned into K subsets. For K repeats, one subset is selected as the "validation set" and the remaining K-1 subsets are iteratively used to train the model and tested against the validation set. The test statistic, misclassification error or deviance, is computed for each repeat and then averaged to provide a single estimate. Using cross validation, it is possible determine λ such that the desired statistic is optimized. Cross validation is included in the glmnet computational package. λ is selected using the "1se" heuristic. This heuristic favours a more parsimonious model where the expected error is within one standard error cross validation error (Friedman et al., 2010) of the minimal error.

Computation of Coefficients—Computation of coefficients in the lasso in the glmnet package is completed using coordinate descent (Friedman et al., 2007, 2010). Parameter estimation and cross-validation is automated as part of the glmnet package (Friedman, Hastie, & Rob, n.d.).

Supplementary Material

Refer to Web version on PubMed Central for supplementary material.

Acknowledgments

This work was funded by the Kane Family Foundation (PRM), Autism Speaks (PRM), the Charles A. Dana Foundation (PRM) and the National Institutes of Health (RO1 DA11723 (PRM), RO1 MH085496 (PRM), T32 NS43124 (KTK) and NRSA F30 MH098571 01 (JTL).

The authors would like to thank the NEMO software development team for their assistance in programming the stimulus presentation scripts, and the Human Neuroimaging Laboratory's technological staff for their assistance with recruitment and scanning

References

Bishop, CM. Pattern Recognition and Machine Learning. New York: Springer Science + Business Media, LLC; 2006. p. 427-450.

Chiu PH, Kayali MA, Kishida KT, Tomlin D, Klinger LG, Klinger MR, Montague PR. Self responses along cingulate cortex reveal quantitative neural phenotype for high-functioning autism. Neuron. 2008; 57(3):463–73.10.1016/j.neuron.2007.12.020 [PubMed: 18255038]

Constantino JN, Todd RD. Autistic traits in the general population: a twin study. Archives of General Psychiatry. 2003; 60(5):524–30.10.1001/archpsyc.60.5.524 [PubMed: 12742874]

Count P. The Lasso Logistic Regression Model: Modifications to aid causality assessment for Adverse Events Following Immunization. Statistics. 2010; 47(September)

Cramer JS. Predictive performance of the binary logit model in unbalanced samples. Journal of the Royal Statistical Society Series D (The Statistician). 2013; 48(1):85–94.

Deeley Q, Daly EM, Surguladze S, Page L, Toal F, Robertson D, Murphy DGM. An event related functional magnetic resonance imaging study of facial emotion processing in Asperger syndrome. Biological Psychiatry. 2007; 62(3):207–17.10.1016/j.biopsych.2006.09.037 [PubMed: 17400195]

Ecker C, Rocha-Rego V, Johnston P, Mourao-Miranda J, Marquand A, Daly EM, Murphy DG. Investigating the predictive value of whole-brain structural MR scans in autism: a pattern classification approach. NeuroImage. 2010; 49(1):44–56.10.1016/j.neuroimage.2009.08.024 [PubMed: 19683584]

Friedman J, Hastie T, Höfling H, Tibshirani R. Pathwise coordinate optimization. The Annals of Applied Statistics. 2007; 1(2):302–332.10.1214/07-AOAS131

Friedman, J.; Hastie, T.; Rob, T. (n.d.). glmnet: Lasso and elastic-net regularized generalized linear models. 2013-03-02. Retrieved April 10, 2013, from http://cran.r-project.org/web/packages/glmnet/index.html

Friedman J, Hastie T, Tibshirani R. Regularization Paths for Generalized Linear Models via Coordinate Descent. Journal Of Statistical Software. 2010; 33(1)

Friston, KJ.; Penny, WD.; Ashburner, JT.; Kiebel, SJ.; Nichols, TE. Statistical parametric mapping: the analysis of funtional brain images. 1. Academic Press; 2006. doi:0123725607

Gray KM, Tonge BJ, Sweeney DJ. Using the Autism Diagnostic Interview-Revised and the Autism Diagnostic Observation Schedule with young children with developmental delay: evaluating diagnostic validity. Journal of Autism and Developmental Disorders. 2008; 38(4):657–67.10.1007/s10803-007-0432-y [PubMed: 17690967]

Grill-Spector K, Henson R, Martin A. Repetition and the brain: neural models of stimulus-specific effects. Trends in Cognitive Sciences. 2006; 10(1):14–23.10.1016/j.tics.2005.11.006 [PubMed: 16321563]

Hadjikhani N, Joseph RM, Snyder J, Chabris CF, Clark J, Steele S, Tager-Flusberg H. Activation of the fusiform gyrus when individuals with autism spectrum disorder view faces. NeuroImage. 2004; 22(3):1141–50.10.1016/j.neuroimage.2004.03.025 [PubMed: 15219586]

Henson RNA, Rugg MD. Neural response suppression, haemodynamic repetition effects, and behavioural priming. Neuropsychologia. 2003; 41(3):263–70. Retrieved from http://www.ncbi.nlm.nih.gov/pubmed/12457752. [PubMed: 12457752]

Huettel, Sa; Song, AW.; McCarthy, G. Functional Magnetic Resonance Imaging. 2. Sinauer Associates; 2008.

Humphreys K, Hasson U, Avidan G, Minshew N, Behrmann M. Cortical patterns of category-selective activation for faces, places and objects in adults with autism. Autism Research: Official Journal of the International Society for Autism Research. 2008; 1(1):52–63.10.1002/aur.1 [PubMed: 19360650]

Jiao Y, Chen R, Ke X, Chu K, Lu Z, Herskovits EH. Predictive models of autism spectrum disorder based on brain regional cortical thickness. NeuroImage. 2010; 50(2):589–99.10.1016/j.neuroimage.2009.12.047 [PubMed: 20026220]

Johnson CP, Myers SM. Identification and evaluation of children with autism spectrum disorders. Pediatrics. 2007; 120(5):1183–215.10.1542/peds.2007-2361 [PubMed: 17967920]

Kanwisher N, Yovel G. The fusiform face area: a cortical region specialized for the perception of faces. Philosophical Transactions of the Royal Society of London Series B, Biological Sciences. 2006; 361(1476):2109–28.10.1098/rstb.2006.1934 [PubMed: 17118927]

Kaufman, ASKN. K-BIT: Kaufman Brief Intelligence Test. American Guidance Service. , editor. Circle Pines, MN: 2004. *American Guidance Services* (Second Edi.)

King-Casas B, Tomlin D, Anen C, Camerer CF, Quartz SR, Montague PR. Getting to know you: reputation and trust in a two-person economic exchange. Science (New York, N.Y). 2005; 308(5718):78–83.10.1126/science.1108062

Kishida KT, King-casas B, Montague PR. Neuroeconomic approaches to mental disorders. Read. 2011; 67(4):543–554.10.1016/j.neuron.2010.07.021.Neuroeconomic

Kishida KT, Li J, Schwind J, Montague PR. New approaches to investigating social gestures in autism spectrum disorder. Journal of Neurodevelopmental Disorders. 2012; 4(1):14.10.1186/1866-1955-4-14 [PubMed: 22958572]

Le Couteur, A.; Lord, C.; Rutter, M. The Autism Diagnostic Interview—Revised (ADI-R). Los Angeles, CA: 2003.

Lichtenstein P, Carlström E, Råstam M, Gillberg C, Anckarsäter H. The genetics of autism spectrum disorders and related neuropsychiatric disorders in childhood. The American Journal of Psychiatry. 2010; 167(11):1357–63.10.1176/appi.ajp.2010.10020223 [PubMed: 20686188]

Lombardo MV, Chakrabarti B, Bullmore ET, Sadek Sa, Pasco G, Wheelwright SJ, Baron-Cohen S. Atypical neural self-representation in autism. Brain: A Journal of Neurology. 2010; 133(Pt 2):611–24.10.1093/brain/awp306 [PubMed: 20008375]

Lord, C.; Rutter, M.; DiLavore, PD.; Risi, S. Autism Diagnostic Observation Schedule. Los Angeles, CA: 2001.

Mitchell P, O'Keefe K. Brief report: do individuals with autism spectrum disorder think they know their own minds? Journal of Autism and Developmental Disorders. 2008; 38(8):1591–7.10.1007/s10803-007-0530-x [PubMed: 18311515]

Neeley ES, Bigler ED, Krasny L, Ozonoff S, McMahon W, Lainhart JE. Quantitative temporal lobe differences: autism distinguished from controls using classification and regression tree analysis. Brain & Development. 2007; 29(7):389–99.10.1016/j.braindev.2006.11.006 [PubMed: 17204387]

Pessoa L, McKenna M, Gutierrez E, Ungerleider LG. Neural processing of emotional faces requires attention. Proceedings of the National Academy of Sciences of the United States of America. 2002; 99(17):11458–63.10.1073/pnas.172403899 [PubMed: 12177449]

Pierce K, Haist F, Sedaghat F, Courchesne E. The brain response to personally familiar faces in autism: findings of fusiform activity and beyond. Brain: A Journal of Neurology. 2004; 127(Pt 12):2703–16.10.1093/brain/awh289 [PubMed: 15319275]

Pierce K, Redcay E. Fusiform function in children with an autism spectrum disorder is a matter of "who". Biological Psychiatry. 2008; 64(7):552–60.10.1016/j.biopsych.2008.05.013 [PubMed: 18621359]

Power JD, Barnes Ka, Snyder AZ, Schlaggar BL, Petersen SE. Spurious but systematic correlations in functional connectivity MRI networks arise from subject motion. NeuroImage. 2012; 59(3):2142–54.10.1016/j.neuroimage.2011.10.018 [PubMed: 22019881]

Ronald A, Happé F, Bolton P, Butcher LM, Price TS, Wheelwright S, Plomin R. Genetic heterogeneity between the three components of the autism spectrum: a twin study. Journal of the American Academy of Child and Adolescent Psychiatry. 2006; 45(6):691–9.10.1097/01.chi.0000215325.13058.9d [PubMed: 16721319]

Sally D, Hill E. The development of interpersonal strategy: Autism, theory-of-mind, cooperation and fairness. Journal of Economic Psychology. 2006; 27(1):73–97.10.1016/j.joep.2005.06.015

Schaaf CP, Zoghbi HY. Solving the autism puzzle a few pieces at a time. Neuron. 2011; 70(5):806–808.10.1016/j.neuron.2011.05.025 [PubMed: 21658575]

Segaert K, Weber K, de Lange FP, Petersson KM, Hagoort P. The suppression of repetition enhancement: a review of fMRI studies. Neuropsychologia. 2013; 51(1):59–66.10.1016/j.neuropsychologia.2012.11.006 [PubMed: 23159344]

Tibshirani R. Regression Shrinkage and Selection via Lasso. Journal of the Royal Statistical Society Series B (Methodological). 1996; 58(1):267–288.

Tomlin D, Kayali MA, King-Casas B, Anen C, Camerer CF, Quartz SR, Montague PR. Agent-specific responses in the cingulate cortex during economic exchanges. Science (New York, N.Y). 2006; 312(5776):1047–50.10.1126/science.1125596

Ventola PE, Kleinman J, Pandey J, Barton M, Allen S, Green J, Fein D. Agreement among four diagnostic instruments for autism spectrum disorders in toddlers. Journal of Autism and Developmental Disorders. 2006; 36(7):839–47.10.1007/s10803-006-0128-8 [PubMed: 16897398]

Wilke M, Holland SK, Altaye M, Gaser C. Template-O-Matic: a toolbox for creating customized pediatric templates. NeuroImage. 2008; 41(3):903–13.10.1016/j.neuroimage.2008.02.056 [PubMed: 18424084]

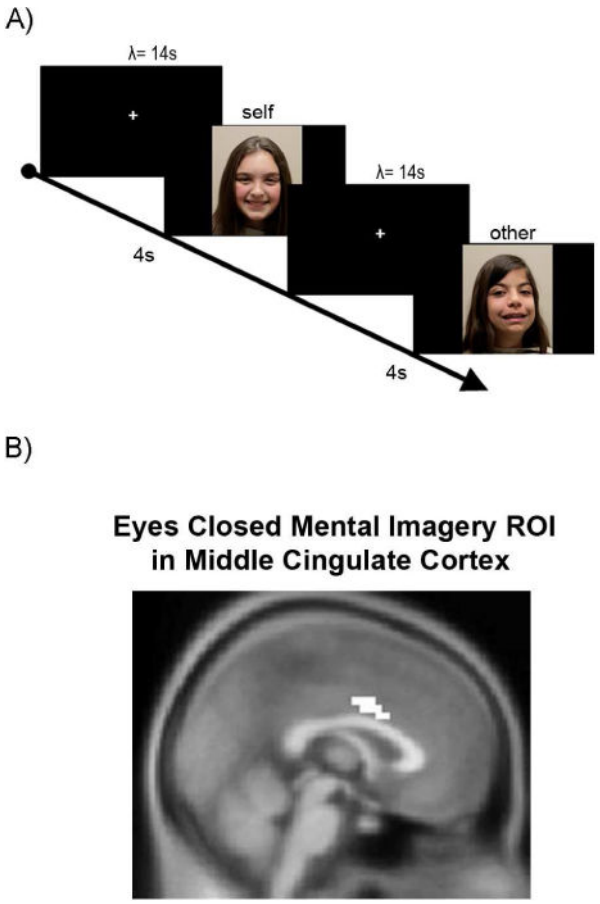

Figure 1.

A) In the scanner, each participant was shown 15 pictures of the subject (‘self’), and 15 unique pictures of a single age-, gender-, and IQ-matched individual (‘other’) for four seconds. Images were shown in random order with Poisson distributed inter stimulus intervals (λ = 14). Demographics are reported in Table S1. **B)** 10 voxel mask from an Eyes-Closed Mental Imagery task (2) defined a region-of-interest in adults (MNI coordinates).

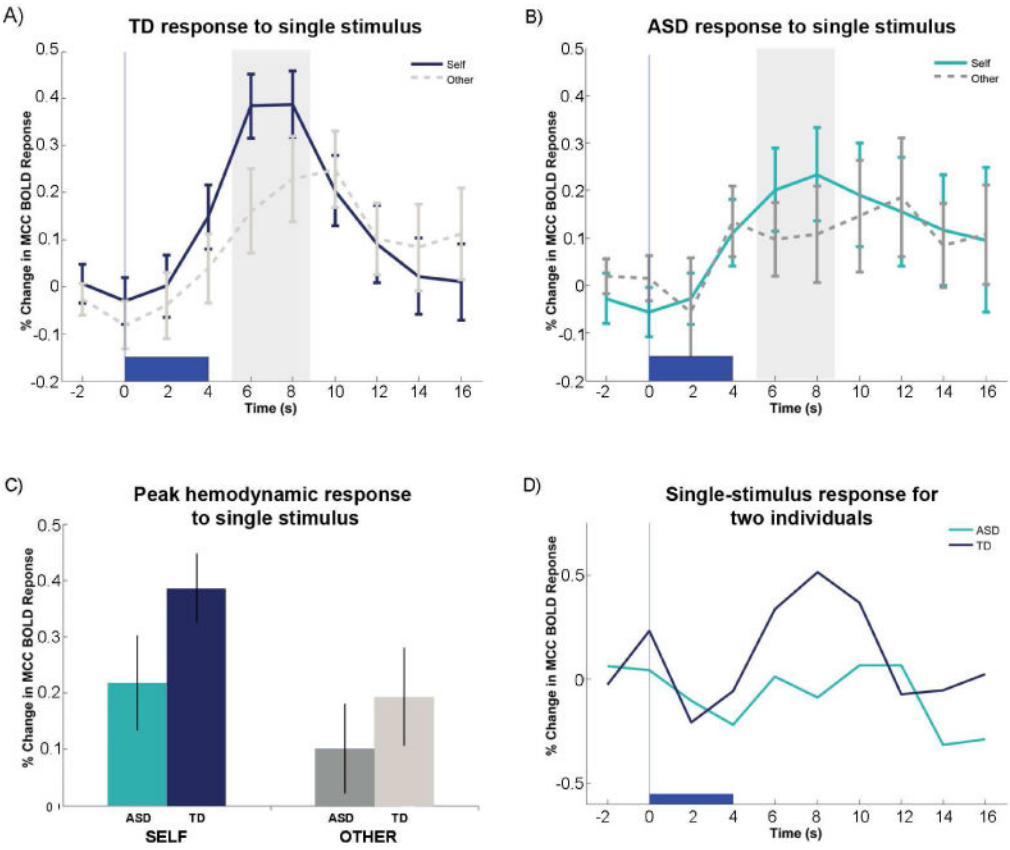

Figure 2.

A) Time series for single stimulus presentation averaged over typically developing (TD) children (n=38), and **B)** Autism Spectrum Disorder (ASD) (n=22) children. **C) Peak** Hemodynamic for ASD and TD for single stimulus “self” and “other” images **D)** Hemodynamic responses to single stimulus self-images for single ASD and TD individuals. Trajectories for all participants can be found in Figure S2.

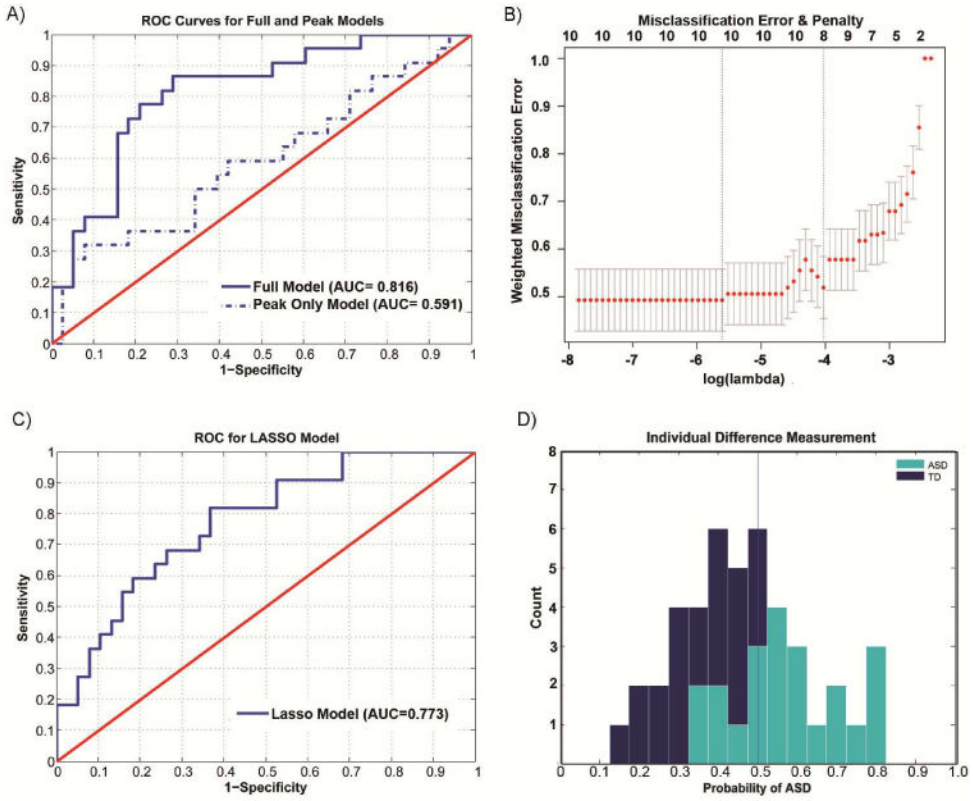

Figure 3.

Differences in BOLD MCC responses to single stimulus "self" images classifies individual subjects. **A)** ROC curves for a 'full' logistic model and a model based on averaging peak responses. B) Misclassification error versus penalization in penalized logistic regression model. Lambda (bottom horizontal axis) is the amount of penalization. The top of the plot shows the number of variables (i.e., degrees of freedom) included in the model as penalization changes. Less penalization, log(λ), results in more degrees of freedom. Two vertical lines are plotted; the left line ("min") is the penalization that produced minimal misclassification error. The right line is the penalization ("1se") that is within one standard cross-validation error of the minimum error. λ is selected using the "1se" rule as the error are statistically equivalent, but the model is more parsimonious **C)** ROC curves for a penalized logistic regression model using a Leave –One – Out Cross Validation. The penalized cross validated model utilizes only data from 8 covariates. **D)** Histograms of Individual Difference measure, *p(status=ASD|M)*, given the penalized model (M). The D' between the ASD and TD cohorts is 1.50 for the single shot measurements and 1.61 for the full model.

Table 1

A)Comparison of coefficients for the full logistic regression model with coefficients from the penalized model. The model is over parameterized; parameters for time since onset (sec)= −2, 0 and 2 cannot be computed with precision. **B)** 2×2 classification table for the cross validated penalized model

A)

		Full Model (logit)			Penalized Model
ID	**Coefficient**	**Estimate**	**Std. Error**	**Pr(>|z|)**	**Estimate**
0	Intercept	2.917	0.937	0.002	1.487
1	Age	−0.216	0.069	0.002	−0.104
2	Start	1.102	0.509	0.030	0.443
3	−2.00	24100	56430	0.669	0.000
4	0 (Presentation)	24100	56430	0.669	0.000
5	2.00	24100	56430	0.669	0.000
6	4.00	5.327	1.358	0.000	1.591
7	6.00	−4.998	1.393	0.000	−2.270
8	8.00	−1.729	1.008	0.086	−0.226
9	10.00	2.345	0.916	0.010	0.362
10	12.00	0.012	0.979	0.991	0.000
11	14.00	0.586	0.726	0.419	0.474
12	16.00	0.301	0.536	0.574	0.122

B)

		Actual		
		ASD	**TD**	**Total**
Prediction	**ASD**	14	10	24
	TD	8	28	36
	Total	22	38	60
	Sensitivity	63.64%	Specificity	73.68%